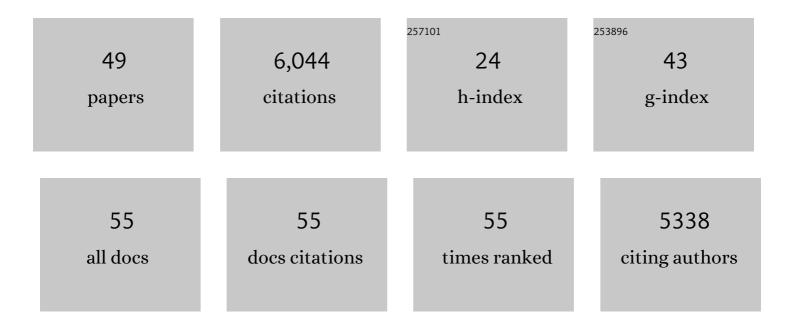
Shigenori Nonaka, é**ž**,-èŒ,ç´€

List of Publications by Year in descending order

Source: https://exaly.com/author-pdf/6268217/publications.pdf Version: 2024-02-01



#	Article	IF	CITATIONS
1	Depletion of Ift88 in thymic epithelial cells affects thymic synapse and T-cell differentiation in aged mice. Anatomical Science International, 2022, , 1.	0.5	1
2	Near-wall rheotaxis of the ciliate <i>Tetrahymena</i> induced by the kinesthetic sensing of cilia. Science Advances, 2021, 7, eabi5878.	4.7	12
3	Colocalization Analysis of Lipo-Deoxyribozyme Consisting of DNA and Protic Catalysts in a Vesicle-Based Protocellular Membrane Investigated by Confocal Microscopy. Life, 2021, 11, 1364.	1.1	3
4	Lightâ€sheet microscopyâ€based 3D singleâ€cell tracking reveals a correlation between cell cycle and the start of endoderm cell internalization in early zebrafish development. Development Growth and Differentiation, 2020, 62, 495-502.	0.6	5
5	Transient microglial absence assists postmigratory cortical neurons in proper differentiation. Nature Communications, 2020, 11, 1631.	5.8	35
6	Developmental analyses of mouse embryos and adults using a non-overlapping tracing system for all three germ layers. Development (Cambridge), 2019, 146, .	1.2	7
7	Evolutionary transformation of mouthparts from particle-feeding to piercing carnivory in Viper copepods: Review andÂ3D analyses of a key innovation using advanced imaging techniques. Frontiers in Zoology, 2019, 16, 35.	0.9	2
8	Calaxin is required for cilia-driven determination of vertebrate laterality. Communications Biology, 2019, 2, 226.	2.0	26
9	System level analysis of motor-related neural activities in larval <i>Drosophila</i> . Journal of Neurogenetics, 2019, 33, 179-189.	0.6	5
10	Skeleton construction upon local regression of the sponge body. Development Growth and Differentiation, 2019, 61, 485-500.	0.6	0
11	Stress-Fiber Wheel Rotation in Keratocytes. Seibutsu Butsuri, 2019, 59, 094-096.	0.0	0
12	Simple mechanosense and response of cilia motion reveal the intrinsic habits of ciliates. Proceedings of the National Academy of Sciences of the United States of America, 2018, 115, 3231-3236.	3.3	39
13	Influence of cellular shape on sliding behavior of ciliates. Communicative and Integrative Biology, 2018, 11, e1506666.	0.6	15
14	Rotation of stress fibers as a single wheel in migrating fish keratocytes. Scientific Reports, 2018, 8, 10615.	1.6	11
15	Axiallyâ€confined <i>inÂvivo</i> singleâ€cell labeling by primed conversion using blue and red lasers with conventional confocal microscopes. Development Growth and Differentiation, 2017, 59, 741-748.	0.6	6
16	Live imaging of primary ocular vasculature formation in zebrafish. PLoS ONE, 2017, 12, e0176456.	1.1	11
17	High-speed microscopy with an electrically tunable lens to image the dynamics ofin vivomolecular complexes. Review of Scientific Instruments, 2015, 86, 013707.	0.6	45
18	Ultrasensitive Imaging of Ca2+ Dynamics in Pancreatic Acinar Cells of Yellow Cameleon-Nano Transgenic Mice. International Journal of Molecular Sciences, 2014, 15, 19971-19986.	1.8	9

#	Article	IF	CITATIONS
19	Wide field intravital imaging by two-photon-excitation digital-scanned light-sheet microscopy (2p-DSLM) with a high-pulse energy laser. Biomedical Optics Express, 2014, 5, 3311.	1.5	17
20	Live imaging and quantitative analysis of gastrulation in mouse embryos using light-sheet microscopy and 3D tracking tools. Nature Protocols, 2014, 9, 575-585.	5.5	48
21	3SDA-04 Live imaging of whole organisms by light-sheet microscopy(Cutting-Edge Optical Imaging) Tj ETQq1 1 ().784314 r 0.0	gBT /Overlo 0
22	Asymmetric distribution of dynamic calcium signals in the node of mouse embryo during left–right axis formation. Developmental Biology, 2013, 376, 23-30.	0.9	62
23	Mechanism of microtubule array expansion in the cytokinetic phragmoplast. Nature Communications, 2013, 4, 1967.	5.8	102
24	Visualization of Mouse Nodal Cilia and Nodal Flow. Methods in Enzymology, 2013, 525, 149-157.	0.4	4
25	Live Imaging of Whole Mouse Embryos during Gastrulation: Migration Analyses of Epiblast and Mesodermal Cells. PLoS ONE, 2013, 8, e64506.	1.1	66
26	Light-Sheet Microscopy for Live Imaging. The Review of Laser Engineering, 2013, 41, 103.	0.0	0
27	Multimodal light-sheet microscopy for fluorescence live imaging. Proceedings of SPIE, 2012, , .	0.8	2
28	Cilia at the Node of Mouse Embryos Sense Fluid Flow for Left-Right Determination via Pkd2. Science, 2012, 338, 226-231.	6.0	262
29	Light sheet-excited spontaneous Raman imaging of a living fish by optical sectioning in a wide field Raman microscope. Optics Express, 2012, 20, 16195.	1.7	50
30	Cell movements of the deep layer of non-neural ectoderm underlie complete neural tube closure in <i>Xenopus</i> . Development (Cambridge), 2012, 139, 1417-1426.	1.2	45
31	High-Speed Imaging of Amoeboid Movements Using Light-Sheet Microscopy. PLoS ONE, 2012, 7, e50846.	1.1	16
32	Migration of neuronal precursors from the telencephalic ventricular zone into the olfactory bulb in adult zebrafish. Journal of Comparative Neurology, 2011, 519, 3549-3565.	0.9	59
33	Planar polarization of node cells determines the rotational axis of node cilia. Nature Cell Biology, 2010, 12, 170-176.	4.6	190
34	Planar polarity of multiciliated ependymal cells involves the anterior migration of basal bodies regulated by non-muscle myosin II. Development (Cambridge), 2010, 137, 3037-3046.	1.2	94
35	Planar cell polarity of multiciliated ependymal cells regulated by non-muscle myosin II. Neuroscience Research, 2010, 68, e364.	1.0	Ο
36	Modification of Mouse Nodal Flow by Applying Artificial Flow. Methods in Cell Biology, 2009, 91, 287-297.	0.5	5

#	Article	IF	CITATIONS
37	Planar polarity decisions for directional beating of ependymal cilia and fluid flow in the adult mouse lateral ventricles. Neuroscience Research, 2009, 65, S54.	1.0	0
38	16-P018 Cell polarity in the node for basal body positioning and nodal flow. Mechanisms of Development, 2009, 126, S267.	1.7	0
39	Cilia: Tuning in to the Cell's Antenna. Current Biology, 2006, 16, R604-R614.	1.8	243
40	De Novo Formation of Left–Right Asymmetry by Posterior Tilt of Nodal Cilia. PLoS Biology, 2005, 3, e268.	2.6	273
41	Notch signaling regulates left-right asymmetry determination by inducing Nodal expression. Genes and Development, 2003, 17, 1207-1212.	2.7	207
42	The left-right determinant Inversin is a component of node monocilia and other 9+0 cilia. Development (Cambridge), 2003, 130, 1725-1734.	1.2	176
43	Determination of left–right patterning of the mouse embryo by artificial nodal flow. Nature, 2002, 418, 96-99.	13.7	596
44	Left-Right Asymmetry and Kinesin Superfamily Protein KIF3A: New Insights in Determination of Laterality and Mesoderm Induction by kif3Aâ~'/â~' Mice Analysis. Journal of Cell Biology, 1999, 145, 825-836.	2.3	419
45	Abnormal Nodal Flow Precedes Situs Inversus in iv and inv mice. Molecular Cell, 1999, 4, 459-468.	4.5	402
46	Targeted Disruption of Mouse Conventional Kinesin Heavy Chain kif5B, Results in Abnormal Perinuclear Clustering of Mitochondria. Cell, 1998, 93, 1147-1158.	13.5	590
47	Randomization of Left–Right Asymmetry due to Loss of Nodal Cilia Generating Leftward Flow of Extraembryonic Fluid in Mice Lacking KIF3B Motor Protein. Cell, 1998, 95, 829-837.	13.5	1,489
48	Golgi Vesiculation and Lysosome Dispersion in Cells Lacking Cytoplasmic Dynein. Journal of Cell Biology, 1998, 141, 51-59.	2.3	330
49	The primary structure of rat brain (cytoplasmic) dynein heavy chain, a cytoplasmic motor enzyme Proceedings of the National Academy of Sciences of the United States of America, 1993, 90, 7928-7932.	3.3	62